Polymer semiconductor crystals

One of the long-standing challenges in the field of polymer semiconductors is to figure out how long interpenetrating and entangled polymer chains self-assemble into single crystals from the solution phase or melt. The ability to produce these crystalline solids has fascinated scientists from a broad range of backgrounds including physicists, chemists, and engineers. Scientists are still on the hunt for determining the mechanism of crystallization in these information-rich materials. Understanding the theory and concept of crystallization of polymer semiconductors will undoubtedly transform this area from an art to an area that will host a bandwagon of scientists and engineers. In this article we describe the basic concept of crystallization and highlight some of the advances in polymer crystallization from crystals to nanocrystalline fibers.

Jung Ah Lim, Feng Liu, Sunzida Ferdous, Murugappan Muthukumar, and Alejandro L. Briseno*
Polymer Science and Engineering Department, University of Massachusetts, Amherst, MA 01003, USA
**E-mail: abriseno@mail.pse.umass.edu*

From a fundamental viewpoint, polymer semiconductor single crystals are critical for understanding the physics of polymer crystallization. They are also important tools for elucidating macromolecular interactions and solid-state packing in benchmark materials, i.e., poly(3-hexylthiophene)(P3HT), and in newly synthesized polymer semiconductors. Knowledge in this area has flourished to a point where structure-property studies have taught and enabled chemists to design materials with tunable properties for a variety of applications. Polymer single crystals are also important for studying intrinsic charge transport and determining the performance limitation of the material in question. These highly organized solids will one day help answer the age-long question regarding the mechanism of charge transport in conjugated polymers[1]. From a technical point of view, polymer crystals may well play an important role in consumer electronic applications such as in flexible displays based on high mobility transistors, solar cells, gadgets and toys, or possibly in technical applications not yet realized by us.

Organic single crystals grown from small-molecule semiconductors have attracted much attention in recent years because of their utilization in both fundamental and applied science[2,3]. However, compared to organic crystals, there is very limited literature on polymer

ISSN:1369 7021 © Elsevier Ltd 2010

semiconductor single crystals or highly crystalline self-assembled nanostructures. These solids are not to be confused with the well established conventional polymer crystals fabricated from soft chain polymers such as polyethylene, which have been recorded in literature for well over 50 years. Polydiacetylenes, a unique family of acetylene-containing polymer chains, are the only known examples of conjugated polymers although it can easily form macroscopic single crystals by polymerization of the crystal of diacetylene monomers[4,5]. This paper, however, focuses on conjugated polymer semiconductors that form highly crystalline solids. To date, a detailed description and mechanism of polymer semiconductor crystallization is still not reported in literature although polymer crystallization has been described by various models and theories for well over 70 years[6-8]. This is because most of the current work on this topic is concentrated on materials such as regioregular poly(3-alkythiophenes), which introduces new parameters that significantly affect the physics of crystallization. For example, these conjugated polymers contain electron-rich backbones and aliphatic chains that have unique handles in crystallization kinetics. The challenge is to get bundles of interpenetrating and entangled conjugated chains to order into a crystal. However, the problem is that polymer crystallization is "frustrated" by the large free energy barriers associated with the reorganization of polymer conformations into ordered states[8]. Nevertheless, the theory and principles of crystallization should be quite applicable to that of these modern polymer semiconductors.

In this article, we discuss a basic concept on polymer semiconductor crystallization. We also highlight some of the recent advances in polymer crystallization with emphasis on single crystals, highly ordered 1-dimensional self-assembled nanostructures, and highly crystalline films. Because the poly(3-alkylthiophenes) (P3ATs) are among one of the most promising and interesting polymer semiconductors to crystallize, we pay close attention to literature work in this article. Since this area of research has produced a large quantity of publications, it is not possible to examine all the interesting breakthroughs in polymer crystallization, at least within the limitation of this context.

Frustration in polymer crystallization

The requisite of morphological purity of polymer crystals fabricated for harnessing the desired electronic properties is commonly faced with the difficult task of polymer crystallization itself. The primary challenge arises from the length of polymer chains that self-assemble into crystals. When collections of interpenetrating chains try to assemble together, the free energy landscape is very rich and there are multiple free energy barriers due to the formation of contacts of monomers (i.e. polymer chains) without significant registry of chain orientations[6,8]. Fig. 1a gives a illustrative description of the free energy landscape for the polymer crystallization process. The troughs correspond to the metastable state in the crystallization process. They come from the competition of several nuclei for the acquisition of monomers or chain segments from polymer chains not yet incorporated into the crystalline phase. The peaks correspond to the energy barrier that separate two metastable states. These barriers are due to the free energy cost involved in the rearrangement of chain conformations originally distributed among many nuclei into fewer nuclei with greater crystalline order. There is a hierarchy of metastable states before the final step of crystallization is reached. This entropic part is further modulated by energy contributions arising from π–π stacking, hydrophobic interactions among the aliphatic chains, and the skeletal bond energies from the local conformation of the chain backbone. Further, since the self-assembled crystal is present in the solution growth medium, there are interfacial energies between the various facets of the crystal and the medium. In order to illustrate the key concepts underlying the spontaneous selection of the morphology of a single crystal grown from solutions, let us consider a crystal prism of lengths L_1, L_2, and L_3, as sketched in Fig. 1b. The molecular interpretation of this sketch is illustrated in Fig. 1c, where a labeled chain can fold several times into a lamella-like organization typical

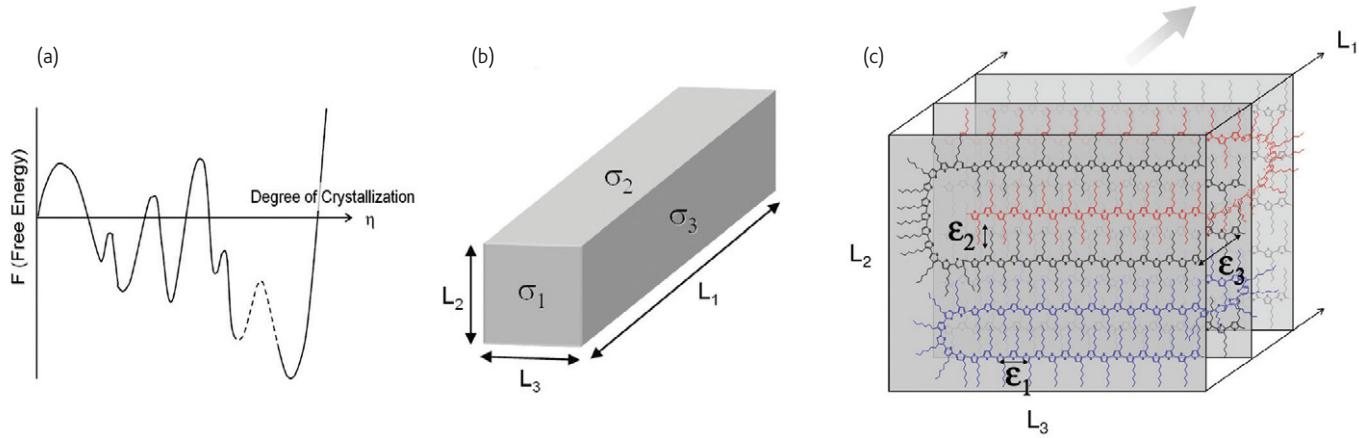

Fig. 1 (a) Sketch of a free energy landscape for polymer crystallization, (b) a 1-D crystal prism labeled with the lengths (L) and interfacial surface energies (σ), and (c) an illustration of the possible self-organized chain packing in a P3HT single crystal labeled with inter- and intramolecular energies (ε).

of polymer crystals. The energy of a bond along the conjugated chain axis is ε_1, while in the orthogonal direction along the crystal axis the energy per a pair of monomers is ε_3, due to π–π stacking. In the other orthogonal direction to the chain axis, the energy per a pair of monomers is ε_2, due to the hydrophobic interactions. Let the interfacial energy of the folded surfaces be σ_3, which arises from both the entropic part associated with the chain folding and the energetic part associated with the polymer-solvent interaction. The corresponding interfacial energies for the end faces (containing aromatic groups, with surface area L_2L_3) and the side faces (containing the aliphatic tails, with surface area L_1L_3) are σ_1 and σ_2, respectively. Theoretical arguments[7] lead to the following result for the equilibrium anisotropy of the crystal as dictated by the above parameters and the following expression:

$$\frac{L_1}{\sigma_1+\frac{\varepsilon_3}{2}}=\frac{L_2}{\sigma_2+\frac{\varepsilon_2}{2}}=\frac{L_3}{\sigma_3+\frac{\varepsilon_1}{2}}$$

Any aspect ratio of the single crystal can thus, in principle, be tuned by designing the chemistry in obtaining the pertinent values of the parameters. The kinetics of the assembly can similarly be controlled by navigating through the free energy landscape, which is also calculated by using the above energy parameters and the chain entropy. We also note that the above parameters can be normalized to accommodate energies associated with templating substrates (e.g. SiO_2).

Polymer semiconductor single crystals

In general, the observed morphology of single [nano] crystals can be correlated to the molecular structure by electron diffraction studies so long as one can acquire the lattice parameters- which can be determined by x-ray crystallography. The geometry of the TEM electron diffraction pattern (i.e. reciprocal lattice points) should in principal correspond to the geometry of the crystal's unit cell (e.g., orthorhombic for P3HT) when viewing down the zone axis. In other words, one should be able to see that the geometry of the reciprocal unit cell resembles the geometry of a rotated real space unit cell. For example, if the *d*-spacing of the (010) and (001) planes can be experimentally determined, then the in-plane unit cell angle (α) can also be easily measured. From these three parameters, one can calculate the *d*-spacing from the equation $rd=L\lambda$; where r is the distance between diffraction spots, d is the spacing between lattice planes, L is the camera length, and λ is the electron wavelength. Moreover, the b and c unit cell values can be determined by the following expression: $|b|=1/(d_{010}\cdot\sin(\alpha))$ and $|c|=1/(d_{001}\cdot\sin(\alpha))$. The consistency of measured values to that of the bulk unit cell dimensions suggest that the molecular or chain packing within the crystal is nearly the same as the bulk crystal structure and therefore the long axis of a 1-D polymer crystal can be accurately elucidated.

Cho and coworkers[9] reported that poly(3-hexylthiophene) (P3HT) (molecular weight (MW)=54 000 g/mol, regioregularity (RR)=98.5%) 1-D microwire single crystals can be grown by the self-seeding method where a dilute P3HT solution in $CHCl_3$ (40°C) is slowly cooled to a crystallization temperature of 10°C over three days. P3HT single crystals grown by this method exhibited well-defined facets and a rectangular cross-section (Fig. 2a). Selected area electron diffraction (SAED) patterns of crystals showed Bragg diffraction spots, not arc-shaped or ring-type diffraction which are often observed from nanostructures with preferred orientation or polycrystalline ordering. The fact that diffraction spots are observed signify that the solid is of single-crystalline nature. It is noteworthy to mention that the P3HT chain axis within the single crystal is perpendicular to the long wire axis and π-π stacking direction is along the crystal growth direction. What is not certain is if the P3HT chains are extended or folded. Preferential π-π stacking in 1-D P3HT single crystals enable charge carrier transport along the wire axis, resulting in high conductivity along the wire direction. In one report, single crystals of poly(3-butylthiophene) (P3BT) (MW=16 000 g/mol, RR=97%) were obtained from solvent mixtures containing a good solvent to provide chain movement and a poor solvent to enhance molecule-molecule interactions[10]. In comparison with the P3HT single crystal, P3BT chains within the single crystal packed normal to the substrate and alkyl side chains were along the crystal growth direction (data not shown). Poly(3-octylthiophene) (P3OT) (MW=120 000 g/mol, RR=98.5%) single crystals were also obtained by a solvent vapor annealing process[11]. It was shown that P3OT chains in a single crystal pack with the polymer backbone parallel to the length of the crystal axis and π-π stacking perpendicular to crystal growth direction (Fig. 2b). The crystal structure was verified by TEM electron diffraction.

More recently, it was shown that self-assembly from dilute solutions can produce single crystal nanowires from a rigid rod polymer semiconductor, a poly(para-phenylene ethynylene) derivative with thioacetate end groups (TA-PPE) (MW=51 318 g/mol)[12]. TA-PPE nanowires exhibited single-crystal diffraction spots and the polymer backbone of TA-PPE chains within the nanowire packed parallel to the nanowire long axis with their side chains vertical to the substrate (Fig. 2c).

Based on these results for polymer semiconductor single crystals, it is proposed that polymer chains in a single crystal have fully extended conformations. However, the packing orientation, crystal morphologies, and relation between crystal growth direction and π-stacking directions appear to be significantly different among polymer materials. This suggests that molecular weight, side chain length, rigidity of chain backbone, and crystal growth conditions such as choice of solvent, all have a profound effect on the crystallization kinetics. Further investigation on the single crystal growth mechanism including origin of nucleation, crystallization kinetics, and interaction between polymer chains will be required. An important question is whether the c-axis of

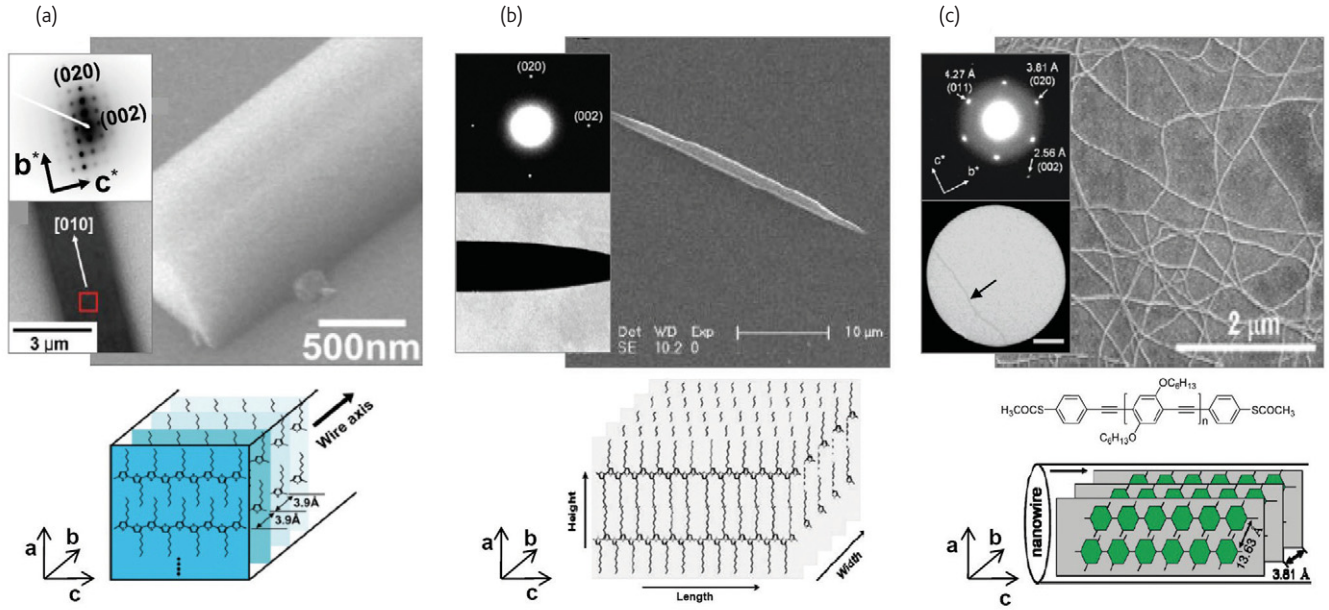

Fig. 2 Field-emission SEM images and SAED patterns for single crystals of (a) poly(3-hexylthiophene) (Reprinted with permission from[9]. ©2006 Wiley-VCH), (b) poly(3-octylthiophene) (Reprinted with permission from[11]. ©2009 American Chemical Society), and (c) thioacetate substituted poly(para-phenylene ethynylene) (Reprinted with permission from[12]. ©2009 American Chemical Society). TEM images for individual crystals along with corresponding SAED analyses are shown in the insets. Schematic illustrations of polymer chain packing in the respective single crystals are also represented below the images.

the polymer chain undergoes chain folding or it remains extended in the solid state. Further investigations will await a better understanding of the nature of chain packing in polymer semiconductor single crystals.

One-Dimensional (1-D) crystalline nanowires

Polymer semiconductors can often have a semi-crystalline nature due to a relatively rigid π-conjugated backbone. Compared to the crystallization of typical insulating polymers such as polyethylene (PE) which form two-dimensional (2-D) lamellar crystals, π-conjugated polymer semiconductors generally crystallize into one-dimensional (1-D) nanostructures, such as nanowires via π-π interactions and via hydrophobic interactions associated with the aliphatic chains[13]. In studies on crystallization kinetics of P3ATs, reported by Nandi and coworkers[14], P3ATs isothermally crystallized into 1-D whiskers, and the Avrami exponent[15] varied in the range of 0.6~1.4, indicating one-dimensional heterogeneous nucleation with linear growth. The Avrami equation, $x(t) = 1\text{-}\exp(-kt^n)$, is a quantitative description of the isothermal crystallization kinetics, where $x(t)$ is the crystallinity developed at time t, k is the overall rate constant, and n is the Avrami exponent denoting the nature of the nucleation and growth process[15].

In general, self-assembly of π-conjugated polymers in a dilute solution under limited solubility can afford highly crystalline 1-D nanowires. At partially soluble conditions, conjugated molecules tend to aggregate in a face-to-face stacking fashion (via π-π interaction between aromatic backbones) in order to decrease unfavorable interaction between the solvent and aromatic main chain[16,17]. In a seminal paper by Ihn and coworkers[18], they reported that P3HT crystallized into nanowhiskers from dilute solution in a poor solvent (i.e. cyclohexanone, n-decane), in which the polymer dissolved only at elevated temperatures. The P3HT nanowhiskers exhibited an average width of 15~20 nm, a length of 10 µm, and a thickness of 5 nm which corresponds to two or three P3HT chain layers (Fig. 3a). X-ray and electron diffraction results confirmed that the P3HT chains pack normal to the long axis of the whisker. Interestingly, P3HT chain folding in a nanowhisker structure was expected because of the considerably greater contour length of P3HT (65 nm for MW 29 000 g/mol) than the whisker width (15nm), although the relatively rigid backbone of P3AT assumed to hamper chain folding. In fact, it has been shown by scanning tunneling microscopy (STM) that the polythiophene backbone can be folded in a planar conformation[19]. The charge carrier mobility in field-effect transistors from a single P3HT nanowire has been reported as high as 0.06 cm^2/Vs which is comparable to that of thin films (~10^{-3} $cm^2/V^{-1}s^{-1}$)[20].

Results of more recent work demonstrated that dimensions of P3HT nanowires can be controlled by varying the molecular weight and concentration of solutions[21]. When the molecular weight of P3HT was less than a critical molecular weight (number average molecular weight (Mn) ~10 kDa), the width of P3HT nanowire corresponded to the length of the extended polymer chain. Whereas for higher molecular weight, the width of nanowire remains constant about 15 nm, regardless of increase in Mn, (Fig. 3b). This result suggested that

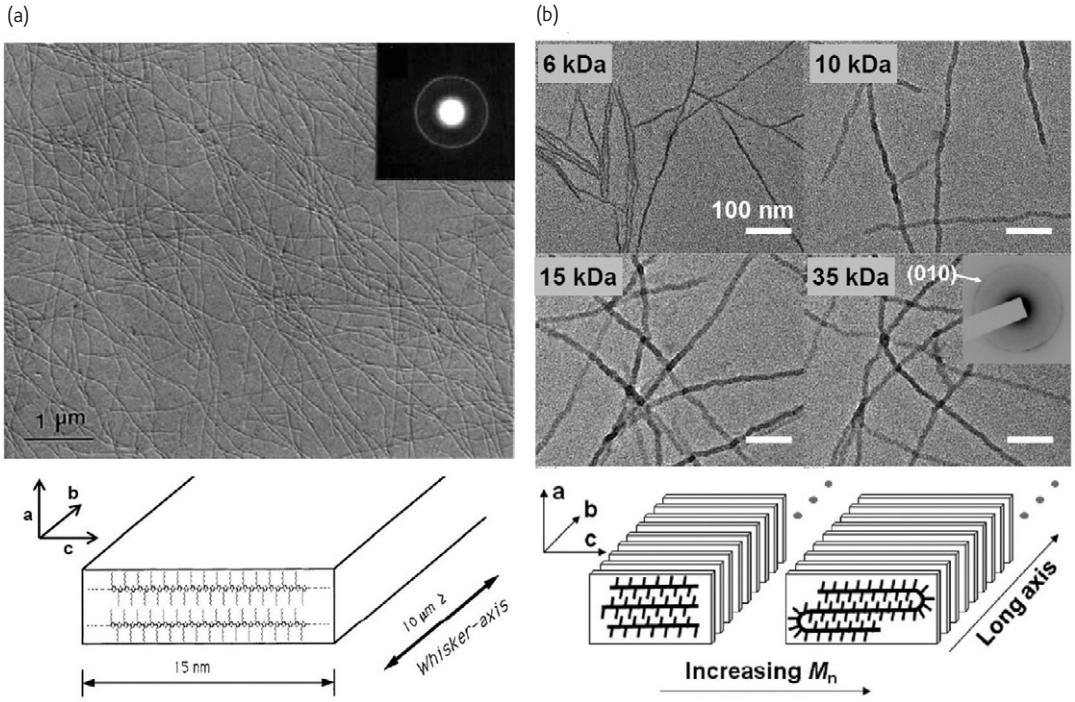

Fig. 3 (a) TEM image of P3HT nanowhiskers crystallized from a cyclohexanone solution and the corresponding schematic representation of the chain arrangement in a nanowire. (inset: corresponding SAED pattern) (Reprinted with permission from[18]. ©1993 American Chemical Society) (b) TEM images of P3HT nanowires and schematic illustration of the extended and folded P3HT backbone packing prepared from low Mn (left) and high Mn (right). (Inset: SAED pattern for P3HT nanowire at molecular weight of 35 kDa) (Reprinted with permission from[21]. ©2009 American Chemical Society).

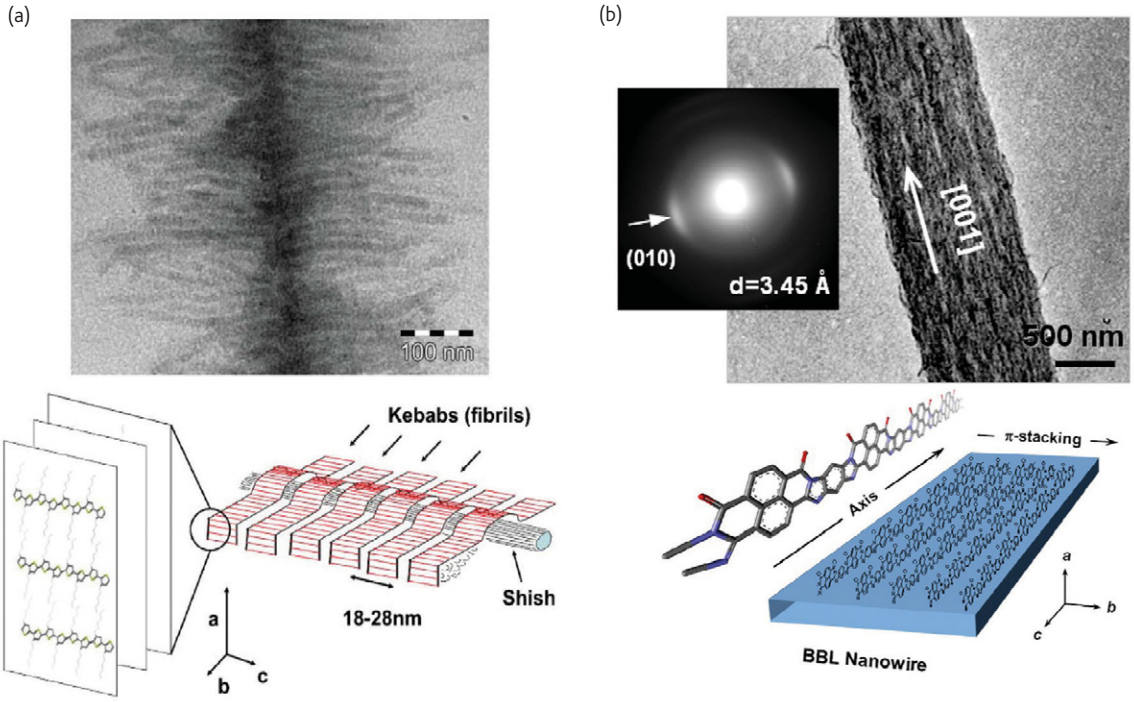

Fig. 4 (a) TEM image of a "shish-kebab" nanofiber of P3HT and a schematic illustration of the shish-kebab chain packing. The P3HT chain is oriented parallel to the fiber axis in shish, and perpendicular to the nanofiber in kebab. (Reprinted with permission from[22]. ©2009 Wiley-VCH) (b) TEM image of an individual BBL nanobelt (inset: the corresponding SAED pattern) and the chain packing of BBL polymer within a nanobelt. (Reprinted with permission from[28]. ©2008 American Chemical Society).

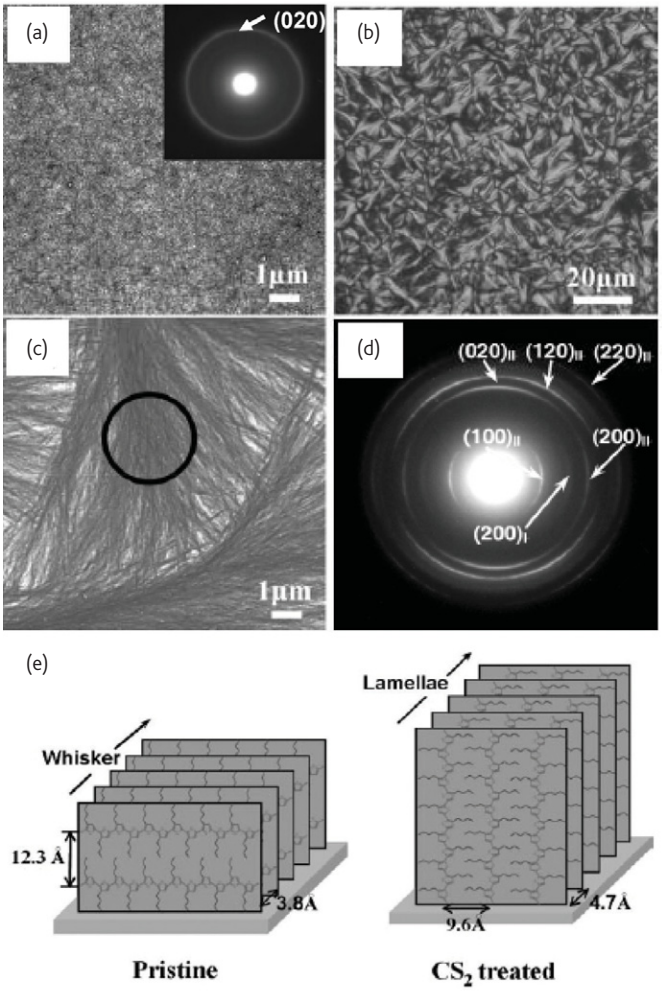

Fig. 5 (a) TEM image of pristine P3BT film spin-coated from an o-dichlorobenzene solution; (b) Polarized light microscopy (PLM) image showing the P3BT film composed of closely contacted spherulites upon CS_2 vapor treatment; (c) TEM image demonstrating the fine structure of the P3BT spherulites and (d) the SAED pattern from the area marked in (c). (e) Schematic illustration of the parallel and perpendicular alignments of P3BT backbones to the substrate, corresponding to "edge-on" and "flat-on" orientations in the conventionally prepared and CS_2-vapor related thin film, respectively. (Reprinted with permission from[30]. ©2007 Wiley-VCH).

conformation of P3HT chain in nanowhisker begins to change from fully extended to folded at a critical Mn. In addition, for fully extended chains (i.e. at low Mn), P3HT nanowires can transform into nanoribbon structures with increased concentration.

Appropriate choices of solvents can also induce unique 1-D nanocrystalline structures. Kiriy and coworkers[17] demonstrated that the addition of hexane into P3AT/chloroform solutions, which is the selective solvent for alkyl side chain but poor solvent for polythiophene backbones, results in 1-D aggregation of P3ATs with helical conformation of main chain. Recently, Brinkmann and coworkers[22] reported that the P3AT nanofibers showing "shish-kebab" morphologies were prepared by epitaxial crystallization in a mixture of 1,3,5-trichlorobenzene (TCB) and a poor solvent of pyridine, as shown in Fig. 4a. In a shish fiber, P3AT chains were oriented parallel to the long axis of TCB needles that were preferably formed in pyridine. In a kebab fibril, folded P3AT chains packed with the pi-stacking direction parallel to the fibril axis.

Formation of 1-D nanowires for various polymer semiconductors, such as polyphenylenevinylenes (PPV), polyfluorenes (PF), poly[(9,9-dioctylfluorenyl-2,7-diyl)-co-(bithiophene)] (F8T2), and poly(3,3'''-didodecyl quarter thiophene) (PQT-12), have also been achieved by self-assembly in a solution with controlled solubilities[23-27]. A recent example of poly(benzobisimidazobenzophenanthroline) (BBL) 1-D nanobelts prepared by self-assembly in solution showed that highly planar and rigid chains pack with fully stretched structures[28]. Unlike polythiophenes, BBL polymer chains preferably packed face-to-face perpendicular to the nanobelt axis without chain folding, as shown in Fig. 4b.

Solvent vapor treatment in a film formation process produces 1-D polythiophene nanowires[29]. P3HT thin films spun-cast under solvent vapor pressure exhibited the nanowire structure (widths of 20~22 nm and heights of 4-5 nm) and nanowire length was controlled by solvent vapor pressure (0~56.5 kPa). It was reported that the crystalline structure and morphology of polythiophene nanowires can be changed by carbon disulfide (CS_2) solvent vapor annealing (Fig. 5)[30]. Pristine P3BT thin films were composed of typical nanowire crystals in which the polythiophene chains pack parallel to the substrate and perpendicular to the long wire axis. However, upon exposure of pristine films to CS_2 vapor, the morphologies of the films significantly evolve from nanowire crystals to spherulites which consist of whiskers radiating from the center. Interestingly, in this whisker crystal, the P3BT chains (c-axis) are oriented perpendicular to the substrate and the whisker grows along the π-π stacking direction (b-axis), as schematically illustrated in Fig. 5e.

Polymer semiconductor copolymers or blends combining different components can be one efficient route to generate self-assembly of polymer semiconductor into 1-D crystalline nanostructures. Diblock copolymer of poly(3-hexylthiophene)-b-poly(styrene), synthesized by McCullough and coworkers, formed well-defined nanowires with a 30-40 nm width that corresponded to the fully extended polythiophene block, as shown in Fig. 6a[31]. For the possible mechanism of this nanowire formation, the core-shell architecture with the polythiophene component constituting the core was expected due to the immiscibility of P3HT and poly(styrene). Nanofibrillar structures have also been found in diblock copolymers of P3HT and rubbery amorphous poly(methyl acrylate)[32]. The transistors based on these nanofibrillar structures exhibited good charge carrier mobilities approaching that of P3HT thin film devices. Jenekhe and coworkers[33] recently demonstrated that crystalline-crystalline diblock co-poly(3-alkylthiophene)s self-assembled into crystalline nanowires, as shown in Fig. 6b. The detailed

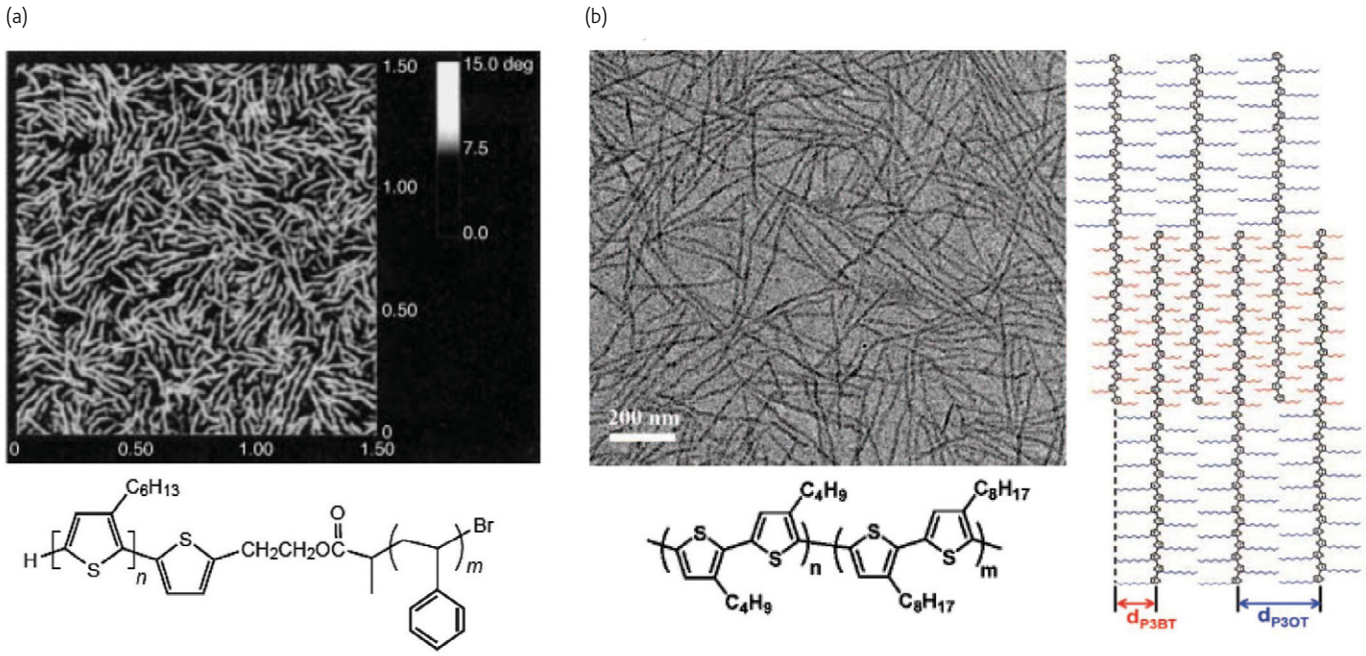

Fig. 6 (a) Tapping mode AFM image (phase) for a poly(3-hexylthiophene)-b-poly(styrene) copolymer thin film prepared from toluene (P3HT fraction: 37%). (Reprinted with permission from[31]. ©2002 Wiley-VCH) (b) TEM image and schematic illustration of lamellar structure of poly(3-butylthiophene)-b-poly(3-octylthiophene) copolymer (P3BT fraction: 50%) (Reprinted with permission from[33]. ©2009 American Chemical Society)

chain packing within the nanowires remains to be investigated, however, they speculate that melt-phase self-assembly of diblock co-poly(3-alkylthiophene)s into lamellar structure has two crystalline domains of the two different side chains. For a blend system, it was reported that polythiophenes/poly(styrene) blend films prepared from selectively marginal solvent for polythiophene component show the polythiophene nanowires embedded in amorphous polystyrene matrix[34,35].

Nanocrystalline thin films

Polymer semiconductor thin films prepared by solution cast processes are composed of both polycrystalline and amorphous domains. Since charge transport in polymer semiconductor thin films is limited by amorphous regions, considerable efforts have been devoted to enhancing crystalline domains. It has been reported that polymer crystallization is strongly depended on molecular weight during the film forming process. There is a speculation that low MW chains find an equilibrium position more easily and produce ordered structures compared to high MW chains because high MW chains have slow crystallization kinetics due to higher viscosity or chain entanglement. McGehee and coworkers[36,37] reported that low MW P3HT (Mn<4 kDa) films form rod-like crystalline nanostructures, while high MW P3HT (Mn>30 kDa) films have isotropic nodule structures with low crystallinity, as shown in Fig. 7a. It is interesting, however, that the field-effect mobilities in transistors increase with increasing MW. It was suggested that the low mobility of low-MW films is probably due to the trapping of charges at the boundaries of rod-like crystalline domains. For the high MW films, it was suggested that crystalline domains are interconnected by the long polymer chains and thus enable more efficient charge transport to occur across grain boundaries. In a separate study, Neher and coworkers[38,39] suggested that P3HT crystalline whiskers from low MW P3HT (Mn<3 kDa) are embedded within a disordered matrix (figure not shown). Neher also proposed that high MW P3HT (Mn>27 kDa) films consist of partially ordered domains in which the chains either fold back, interconnect to neighboring domains, or extend into a disordered phase. McCullough and coworkers[40] also demonstrated that the charge carrier mobilities in transistors fabricated from well-ordered P3HT films increase exponentially with nanofiber width which corresponds to the weight average contour length of polymer chains with Mn ranging from 2 to 13 kDa. The propensity of molecular weight dependency on crystallinity and charge transport properties has also been observed for poly(2,5-bis(alkylthiophen-2-yl)thieno[3,2-b]thiophene) (PBTTT) synthesized by McCulloch and coworkers[41,42]. Higher molecular weight PBTTT (Mn~30 kDa) exhibited a more three-dimensional microstructure with larger crystalline domains and resulted in one of the highest charge carrier mobilities reported to date (0.2-0.6 $cm^2V^{-1}s^{-1}$).

A variety of polymer semiconductors have solubilizing side chains attached to the infusible conjugated backbone to improve solution processability. The crystallization of these polymer semiconductors can be affected by side chain structures. Bao and coworkers[43] and later Sirringhaus and coworkers[44] reported that P3HT chain orientation

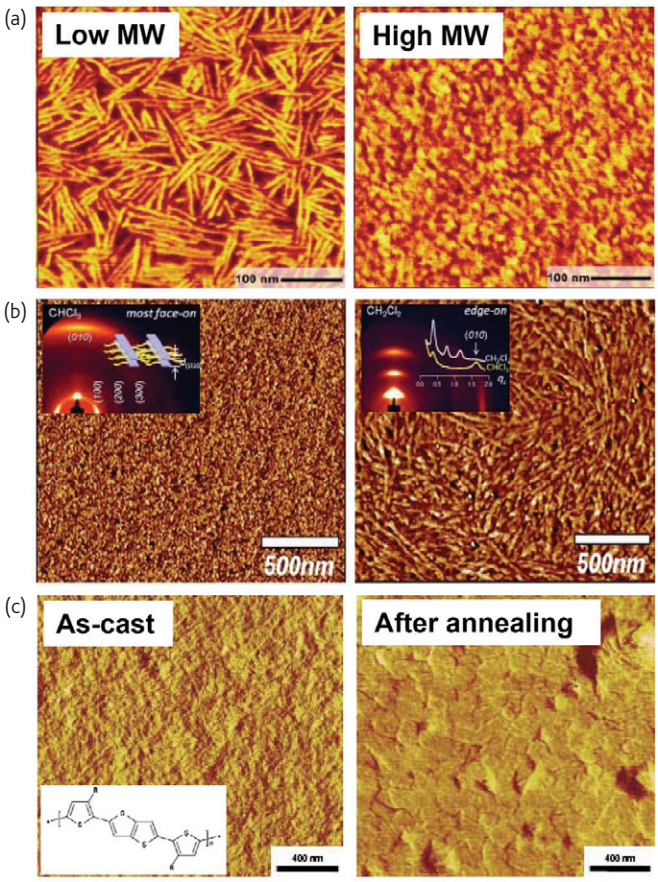

Fig. 7 (a) Tapping mode AFM images (phase) of P3HT thin films with different molecular weight; 3.2 kDa (left) and 31.1 kDa (right). Films were prepared by spin-casting from chloroform. (Reprinted with permission from[36]. ©2003 Wiley-VCH) (b) AFM topographs and grazing incident x-ray diffraction patterns (GIXRD) for P3HT thin films spin-casted from chloroform (left) and methylene chloride (right). GIXRD pattern for chloroform indicates the face-on chain conformation, while for the methylene it shows the edge-on conformations against the substrate. (Reprinted with permission from[47]. ©2007 American Institute of physics) (c) AFM images (phase) of poly(2,5-bis(alkylthiophen-2-yl)thieno[3,2-b]thiophene) (pBTTT) before (left) and after (right) annealing at 180°C. (Inset: chemical structure of pBTTT ($R=C_{12}H_{25}$)) (Reprinted with permission from[42]. ©2006 Nature Publishing Group).

in crystallites was affected by regioregularity of hexyl side chains. In P3HT films with high regioregularity (>91%), the crystallites were preferentially oriented with (100) axis normal to the film and the (010) axis in the plane of the film, often referred to as "edge-on". In contrast, the chain orientation in low regioregular P3HT films (81%) showed the (100) axis in the plane and the (010) axis normal to the film, referred to as "face-on"[44]. There are also reported cases where sufficiently low side chain attachment densities (e.g., PBTTT, PQT-12) permit strategic interdigitation of side chains. DeLongchamp and coworkers[45] suggested that side chain interdigitation of these materials provides a three dimensional chain ordering, and results in high charge transport properties in the films.

The crystalline structures in polymer semiconductor thin films significantly depend on how films are prepared, solvent choice, and post treatment of thin film deposition. For instance, rapid evaporation of solvents can reduce the time to enable highly order films. Sirringhaus and coworkers[46] reported that by using higher boiling point solvents, i.e. 1,2,4-trichlorobenzene (213°C), P3HT films with highly ordered crystalline fibrils were obtained. Furthermore, Yang and coworkers[47] reported that the orientation of P3HT crystallites were dependent on boiling point of solvents, solubility of polymer to solvent, and specific deposition conditions. When P3HT films were prepared from marginal (partially soluble at room temperature) low boiling point solvents such as methylene dichloride (40°C), highly crystalline nanofibrillar structures with edge-on orientation were observed (Fig. 7b). These nanostructured films were prepared by both rapid (spin-coat) and slow (drop-cast) solvent drying methods. Further enhancement of structural order in polymer semiconductor thin films can be obtained through post-deposition annealing. In particular, for polymer semiconductors with liquid crystalline (LC) characteristics, such as PBTTT, PQT-12, poly(didodecylquaterthiophene-alt-didodecylbithiazole), annealing the films above the liquid crystal transition temperature forms large crystalline domains[42,48,49]. A representative example of annealing effects of PBTTT thin films is shown in Fig. 7c[42]. Nodule-like structures of as-prepared films were transformed into large polycrystalline domains with 200 nm diameter grains by annealing at 180°C. More recently, it was reported that PBTTT annealed at the second transition temperature (240°C) exhibited unique crystal shape of terraced nanoscale ribbons[50]. In the case of poly(9,9'-n-dioctylfluorene-alt-bithiophene) (F8T2) deposited on a mechanically rubbed polyimide, annealing of the film in the LC phase attributed to the chain alignment along the rubbing direction of the underlying polyimide[51].

Self-assembly of polymer semiconductor thin films can be governed by the interplay between polymer-polymer interactions and polymer-substrate interactions. Several groups have reported that treating the substrate surface with self-assembled monolayers (SAMs) can significantly vary the crystallite orientation[52-58]. McGehee and coworkers[53] found that octadecyltrichlorosilane (OTS) treatment of silicon dioxide surfaces yields a preferred orientation of P3HT crystallites for in-plane charge transport at the buried interface compared to hexamethyldisilizane (HMDS) treated substrates which yields misoriented crystallites (Fig. 8). Rocking curve analysis was used to determine that crystallites nucleate at substrate-polymer interfaces and also to determine the degree of misorientation of crystallites from both HMDS and OTS treated substrates. In several reports, increased charge carrier mobilities in transistors from several polymer semiconductors, such as P3HT, PQT-12, PBTTT, F8T2, were investigated by various SAM treatments among which OTS treated substrate gave the highest mobilities[54-58]. For PQT-12, this enhanced charge mobility was attributed to an edge-on orientation of PQT-12 crystalline domains induced by the OTS layer[57]. Edge-on orientation gives rise to two-dimensional charge transport caused by efficient π-π stacking in

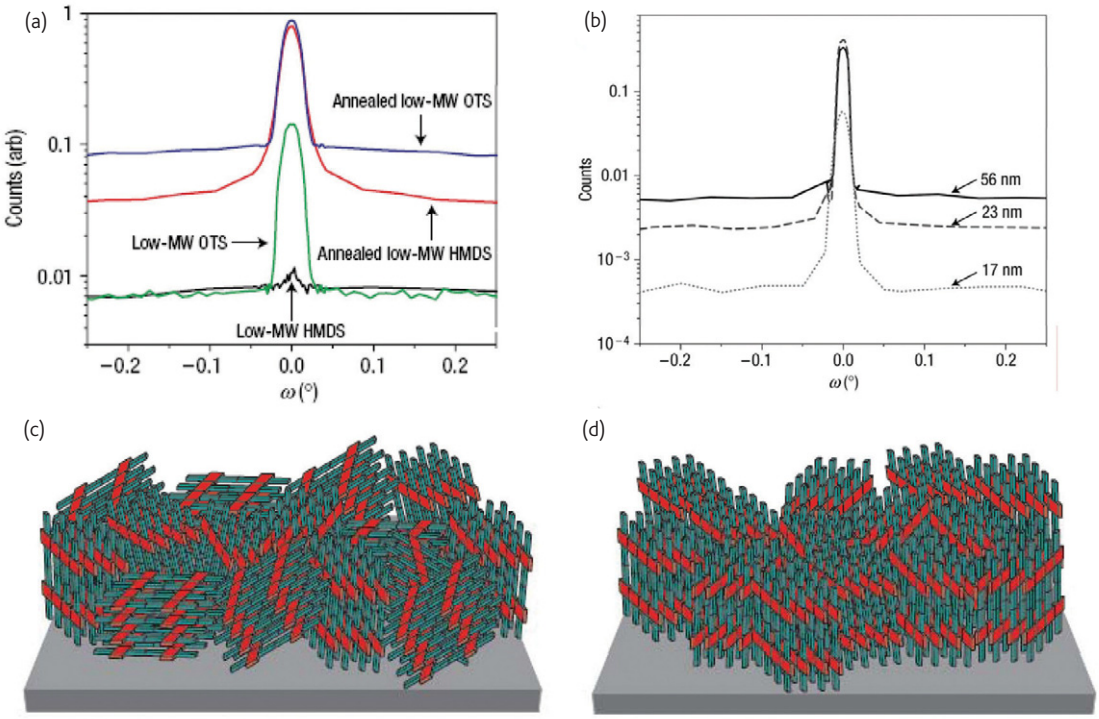

Fig. 8 Rocking curves at (100) diffraction peaks for the spin-casted P3HT films with low molecular weight (a) before and after annealing for both HMDS and OTS-treated substrates and (b) for various film thicknesses on OTS-treated substrate. Proposed schematic of low molecular weight P3HT film with packing arrangements at the buried interface (c) for the film on HMDS treated-substrate; grain boundaries contact with a (100) face and (d) for the film on OTS treated substrate; grain boundaries contact with (010) and (001) faces. (Reprinted with permission from[53]. ©2006 Nature Publishing Group).

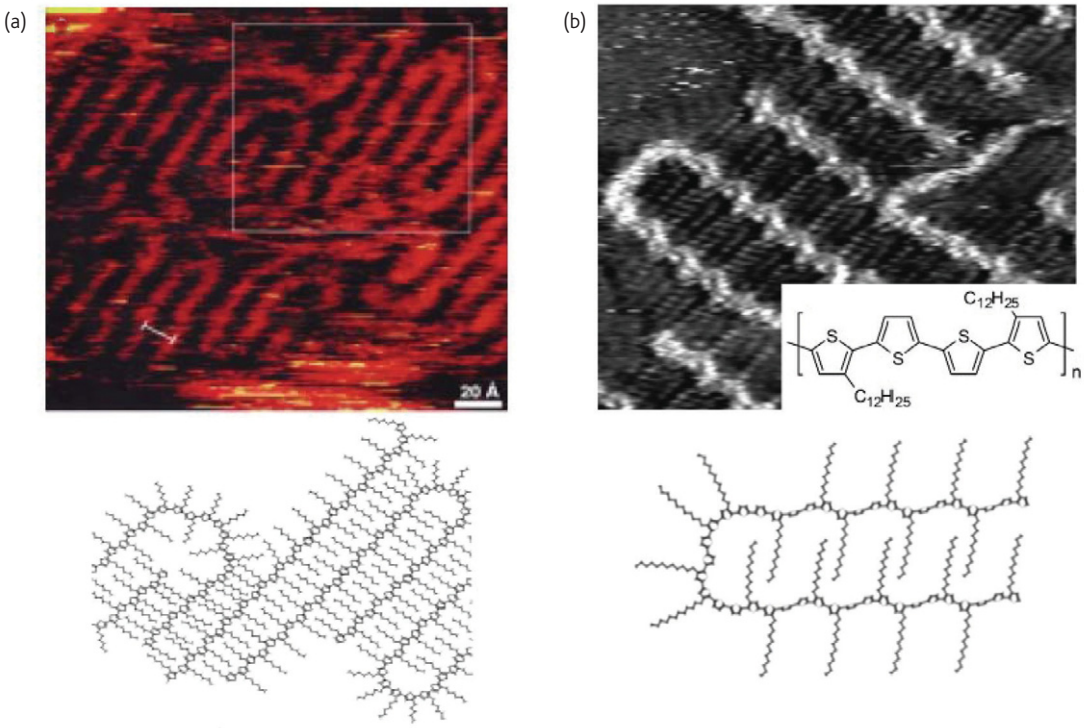

Fig. 9 (a) STM images (200 Å×200 Å) of a short range ordering of P3HT on HOPG. The chain-to-chain distance corresponds to 13-14 Å. The molecular packing corresponding to white square is shown under the image. (Reprinted with permission from[19]. ©2000 Wiley-VCH) (b) STM image of alkyl chain interdigitation of PQT-12 on HOPG and Proposed schematic of chain folding resulting for the U-shaped segments. (Reprinted with permission from[60]. ©2008 Wiley-VCH).

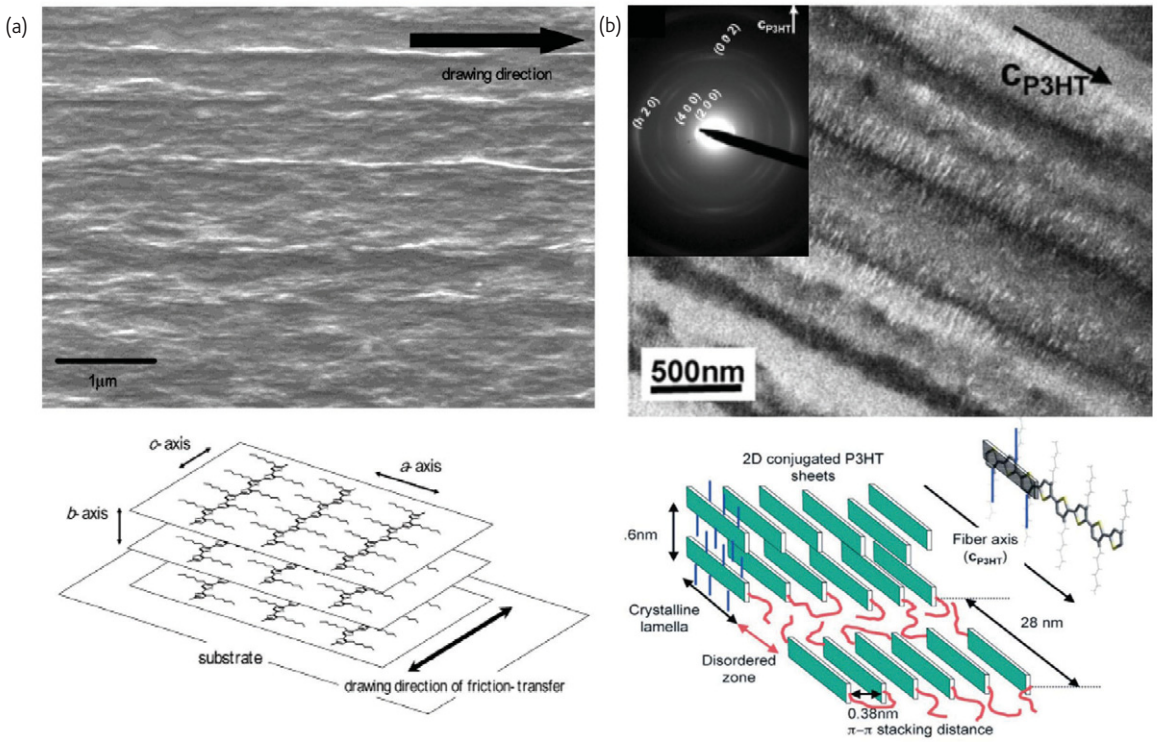

Fig. 10 (a) SEM image of the friction-transferred P3HT film on silicon substrate and schematic of packing arrangement. (Reprinted with permission from[64]. ©2003 American Chemical Society) (b) Dark field TEM image of P3HT film oriented by directional solidification method obtained by selecting the intense 020 reflection. The crystalline lamellae appear bright. (inset: corresponding electron diffraction). Schematic model for organization of the semicrystalline P3HT is represented under the image. (Reprinted with permission from[67]. ©2006 Wiley-VCH).

a parallel direction to the substrate. In contrast, for PBTTT, crystalline domain have similar molecular packing structure on both OTS-treated and untreated SiO_2 surfaces. However, OTS treated surface gives larger domain size and reduce grain boundaries compared to that on SiO_2 surfaces[58].

Two-dimensional crystalline domains of polymer semiconductors have also been studied on highly oriented pyrolytic graphite (HOPG) surfaces[19,59,60]. The HOPG surface facilitates epitaxial growth of these polymers via interaction with alkyl chains. The driving force for this is the alignment of alkyl chains by van der Waals interaction in a planar, interdigitated, zigzag way with the HOPG crystallographic axes, hence guiding the placement of the main chain. Two-dimensional (2-D) crystallization of P3ATs at solution/HOPG interface was observed by means of STM[19]. In this study, conjugated chain folding of P3ATs was clearly visualized, as shown in (Fig. 9a). Calculations based on this image confirmed that a folded chain has *cis*-conformation. STM analysis of P3HT films casted on HOPG exhibited that crystalline mono domains were interconnected by folded chains[59]. More recently, interdigitation of alkyl side chains of polythiophene semiconductor was directly observed for self-assembly of PQT-12 on HOPG surface (Fig. 9b)[60]. Studies on crystallization of poly(dioctylbithiphene-alt-fluorenone) (PDOBTF) on HOPG exhibited less chain folding due to a more rigid backbone compared to P3ATs[61].

Improved chain orientations have been achieved by other methods such as friction transfer, mechanical rubbing and directional epitaxial solidification. P3HT and polyfluorenes (PF) have been employed on friction transferred poly(tetraflouroethylene) (PTFE) surfaces with uniaxially aligned nanoscale ridges[62,63]. The polymer chains aligned along the PTFE friction transfer directions. Friction transferred P3AT films onto substrates exhibited a well-ordered chain backbone along the transfer direction with alkyl side chains lying in the film plane (Fig. 10a)[64]. Analogous to this approach, mechanical rubbing of P3HT films aligned the chain backbone along the sliding direction[65,66]. Brinkmann and coworkers[67] demonstrated directional epitaxial solidification of P3HT by using a crystallizable solvent, 1,3,5-trichlorobenzene (TCB). Crystallization of P3HT occurred at the TCB crystal surface where the chain direction (c_{P3HT}) is parallel to long needle axis of TCB crystals (c_{TCB}) and forms fibrous morphology (Fig. 10b). Using P3HT films fabricated by this technique, Salleo and coworkers[68] demonstrated that the energy barrier for charge transport at crystallite boundaries along a fibril (c_{P3HT}) is relatively small compared to fiber-fiber grain boundaries. More recently, Samitsu and coworkers[69] reported that unidirectional alignment of PQT-12 nanofibers is obtained by anisotropic crystallization in a nematic liquid crystal matrix. Liquid crystal ordering induces polymer chain alignment along the nematic direction.

Summary and outlook

Polymer semiconductor crystallization has been a major challenge for several years now. The phenomenon of crystallization is significantly different than that of small molecules and from traditional "soft" polymers such as polyethylene. Frustration in polymer semiconductor crystallization is attributed to the multiple free energy barriers associated with the cost of polymer conformational changes to reach ordered states. A simple formulation has been described in this paper which takes into account the energy contributions from π–π stacking, skeletal bond energies, hydrophobic interactions, and interfacial energies from solution growth mediums. By combining this mathematical expression with high level molecular modeling and with the modern availability of sensitive experimental techniques, one could piece together the mechanism of polymer semiconductor crystallization. Such a heroic effort will require collaboration between physicists, chemists, and engineers. Fortunately, most of the results towards this goal are becoming available, as highlighted from the elegant studies exposed in this review.

There is only a hand full of reports that have demonstrated true growth of polymer single crystals. Perhaps the use of low molecular weight polymers may yield better crystal growth success since the crystallization kinetics of low molecular weight polymers may very well resemble the free energy landscape of small molecule crystallization where fewer energy barriers exist and frustration is essentially non-existent. This is a particularly exciting time for researchers in the field of polymer semiconductors to apply the facts and theories of crystallization and formulate a protocol for growth of polymer crystals. mt

Acknowledgement

The authors acknowledge support by the NSF Materials Research Science and Engineering Center on Polymers at UMass Amherst (DMR-0820506), and the Center for Hierarchal Manufacturing (CMMI-0531171).

REFERENCES

1. Bredas, J. L., and Street, G. B., *Acc. Chem. Res.* (1985) **18** (10), 309.
2. de Boer, R. W. I., *et al., Phys. Status Solidi a-Appl. Res.* (2004) **201** (6), 1302.
3. Briseno, A. L., *et al., Nature* (2006) **444** (7121), 913.
4. Young, R. J., *et al., Faraday Discuss. Chem. Soc.* (1979) **68**, 509.
5. Thakur, M., and Meyler, S., *Macromolecules* (1985) **18** (11), 2341.
6. Muthukumar, M., *Eur. Phys. J. E* (2000) **3** (2), 199.
7. Rice, S. A., *Advances in Chemical Physics*, John Wiley & Sons, Inc. (2004), 128, Ch. 1.
8. Muthukumar, M., *Lecture Notes in Physics* (2007) **714**, 1.
9. Kim, D. H., *et al., Adv. Mater.* (2006) **18** (6), 719.
10. Ma, Z. Y., *et al., Polymer* (2007) **48** (1), 31.
11. Xiao, X. L., *et al., J. Phys. Chem. B* (2009) **113** (44), 14604.
12. Dong, H. L., *et al., J. Am. Chem. Soc.* (2009) **131** (47), 17315.
13. Briseno, A. L., *et al., Materials Today* (2008) **11** (4), 38.
14. Malik, S., and Nandi, A. K., *J. Polym. Sci. Part B-Polym. Phys.* (2002) **40** (18), 2073.
15. Cheng, S. Z. D., and Wunderlich, B., *Macromolecules* (1988) **21** (11), 3327.
16. Goto, H., *et al., Macromolecules* (2002) **35** (12), 4590.
17. Kiriy, N., *et al., Nano Lett.* (2003) **3** (6), 707.
18. Ihn, K. J., *et al., J. Polym. Sci. Part B-Polym. Phys.* (1993) **31** (6), 735.
19. Mena-Osteritz, E., *et al., Angew. Chem. -Int. Ed.* (2000) **39** (15), 2680.
20. Merlo, J. A., and Frisbie, C. D., *J. Polym. Sci. Part B-Polym. Phys.* (2003) **41** (21), 2674.
21. Liu, J. H., *et al., Macromolecules* (2009) **42** (24), 9390.
22. Brinkmann, M., *et al., Adv. Funct. Mater.* (2009) **19** (17), 2759.
23. Samitsu, S., *et al., Macromolecules* (2008) **41** (21), 8000.
24. Samitsu, S., *et al., Thin Solid Films* (2008) **516** (9), 2478.
25. Samori, P., *et al., Opt. Mater.* (1998) **9** (1-4), 390.
26. Grenier, C. R. G., *et al., Angew. Chem. -Int. Ed.* (2007) **46** (5), 714.
27. Simmonds, H., *et al.,J. Vac. Sci. Technol. B* (2009) **27** (2), 831.
28. Briseno, A. L., *et al., Chem. Mater.* (2008) **20** (14), 4712.
29. Kim, D. H., *et al., Macromol. Rapid Commun.* (2005) **26** (10), 834.
30. Lu, G. H., *et al., Adv. Mater.* (2007) **19** (21), 3594.
31. Liu, J. S., *et al., Angew. Chem. -Int. Ed.* (2001) **41** (2), 329.
32. Sauve, G., and McCullough, R. D., *Adv. Mater.* (2007) **19** (14), 1822.
33. Wu, P. T., *et al., Macromolecules* (2009) **42** (7), 2317.
34. Lu, G. H., *et al., Macromolecules* (2007) **40** (18), 6579.
35. Qiu, L. Z., *et al., Adv. Mater.* (2009) **21** (13), 1349.
36. Kline, R. J., *et al., Adv. Mater.* (2003) **15** (18), 1519.
37. Kline, R. J., et al., Macromolecules (2005) **38** (8), 3312.
38. Zen, A., *et al., Adv. Funct. Mater.* (2004) **14** (8), 757.
39. Zen, A., *et al., Macromolecules* (2006) **39** (6), 2162.
40. Zhang, R., *et al., J. Am. Chem. Soc.* (2006) **128** (11), 3480.
41. McCulloch, I., *et al., Adv. Mater.* (2009) **21** (10-11), 1091.
42. Mcculloch, I., *et al., Nat. Mater.* (2006) **5** (4), 328.
43. Bao, Z., *et al., Appl. Phys. Lett.* (1996) **69** (26), 4108.
44. Sirringhaus, H., *et al., Nature* (1999) **401** (6754), 685.
45. Kline, R. J., *et al., Macromolecules* (2007) **40** (22), 7960.
46. Chang, J. F., *et al., Chem. Mater.* (2004) **16** (23), 4772.
47. Yang, H. H., *et al., Appl. Phys. Lett.* (2007) **90** (17), 172116.
48. Ong, B. S., *et al., Adv. Mater.* (2005) **17** (9), 1141.
49. Kim, D. H., *et al., J. Am. Chem. Soc.* (2009) **131** (17), 6124.
50. DeLongchamp, D. M., *et al., ACS Nano* (2009) **3** (4), 780.
51. Sirringhaus, H., *et al., Appl. Phys. Lett.* (2000) **77** (3), 406.
52. Kim, D. H., *et al., Adv. Funct. Mater.* (2005) **15** (1), 77.
53. Kline, R. J., *et al., Nat. Mater.* (2006) **5** (3), 222.
54. Majewski, L. A., *et al., Appl. Phys. Lett.* (2006) **88** (22), 222108.
55. Sirringhaus, H., *et al., Science* (1998) **280** (5370), 1741.
56. Salleo, A., *et al., Appl. Phys. Lett.* (2002) **81** (23), 4383.
57. Wu, Y., *et al., Appl. Phys. Lett.* (2005) **86** (14), 142102.
58. Chabinyc, M. L., *et al., J. Am. Chem. Soc.* (2007) **129** (11), 3226.
59. Grevin, B., *et al., Adv. Mater.* (2003) **15** (11), 881.
60. Keg, P., *et al., Macromol. Rapid Commun.* (2008) **29** (14), 1197.
61. Brun, M., *et al., Adv. Mater.* (2004) **16** (23-24), 2087.
62. Amundson, K. R., *et al., Thin Solid Films* (2002) **414** (1), 143.
63. Brinkmann, M., *et al., Macromolecules* (2009) **42** (21), 8298.
64. Nagamatsu, S., *et al., Macromolecules* (2003) **36** (14), 5252.
65. Heil, H., *et al., J. Appl. Phys.* (2003) **93** (3), 1636.
66. Derue, G., *et al., J. Am. Chem. Soc.* (2005) **127** (22), 8018.
67. Brinkmann, M., and Wittmann, J. C., *Adv. Mater.* (2006) **18** (7), 860.
68. Jimison, L. H., *et al., Adv. Mater.* (2009) **21** (16), 1568.
69. Samitsu, S., *et al., Macromolecules* (2009) **42** (13), 4366.